JOURNAL OF SOLID STATE CHEMISTRY **107**, 327–331 (1993)

On the Intermediate Valence of Ternary Silicides $CeRhSi_2$ and $CeIrSi_2$

B. CHEVALIER,* P. ROGL,† K. HIEBL,† AND J. ETOURNEAU*

**Laboratoire de Chimie du Solide du CNRS, Université de Bordeaux I, 351 Cours de la Libération, 33405 Talence, France; †Institute of Physical Chemistry, University of Vienna, A-1090 Wien, Währingerstrasse 42, Austria*

Received September 28, 1992; accepted February 24, 1993

$CeRhSi_2$ and $CeIrSi_2$ crystallize in the orthorhombic $CeNiSi_2$-type structure. Magnetic susceptibility and electrical resistivity measurements reveal that cerium in each of these compounds is in an intermediate valence state, but also that the spin fluctuation temperature is much higher for $CeIrSi_2$ than that observed for $CeRhSi_2$. The magnetic behavior of the ternary silicides such as CeM_2Si_2, $Ce_2M_3Si_5$, $CeMSi_3$, and $CeMSi_2$ with M = Rh or Ir depends on the average distance Ce–M which determine the strength of the $4f$(Ce)–$4d$ or –$5d$(M) hybridization. © 1993 Academic Press, Inc.

I. Introduction

We have reported previously on the existence of the ternary silicides $REMSi_2$ (RE = La, Ce, Nd, Sm, Gd and M = Rh, Ir) crystallizing in the orthorhombic $CeNiSi_2$-type structure (*1*). These compounds containing lanthanum show superconductivity below 3.4 K and 2.0 K for $LaRhSi_2$ and $LaIrSi_2$ respectively (*1*, *2*).

In this paper, we study in detail the magnetic and electrical properties of the ternary cerium silicides $CeRhSi_2$ and $CeIrSi_2$. Moreover, we establish a relation between the average distance Ce–M and the physical properties of the compounds $Ce_xM_ySi_z$ observed in the system cerium–rhodium or iridium–silicon such as CeM_2Si_2, $Ce_2M_3Si_5$, and $CeMSi_3$ (M = Rh or Ir).

II. Experimental

$CeRhSi_2$ and $CeIrSi_2$ have been prepared by direct melting of the elements in an arc furnace under a purified argon atmosphere followed by annealing treatment at 900°C for one week. The samples have been examined by conventional X-ray diffractometry, using a Guinier camera (Cu$K\alpha$). Microprobe analysis has been used to check the homogeneity and the composition of the obtained materials.

Magnetic susceptibility measurements have been performed in the temperature range 4.2–150 K using a SQUID magnetometer, and for higher temperatures 77–1000 K with a Faraday balance. The electrical properties have been investigated above 4.2 K by resistivity measurements, using a four-probe DC technique.

III. Results and Discussion

The analysis of the samples, performed by electron microprobe technique and based on the measurements of the Ce$L\alpha$, Rh$L\alpha$, Ir$L\alpha$, and Si$K\alpha$ X-ray radiations, indicated by comparison with $CeRh_2Si_2$ and $CeIr_2Si_2$ silicides used as standard, that they are obtained as a single phase. The results of this analysis of $CeRhSi_2$ (Ce: 25.4(2)%; Rh: 24.6(2)%; Si: 50.0(2)% given in atomic percentage) or on $CeIrSi_2$ (Ce: 25.4(3)%; Ir:

0022-4596/93 $5.00

TABLE I

CRYSTALLOGRAPHIC DATA AND AVERAGE Ce–M, Ce–Si DISTANCES AND CERIUM VALENCE FOR RHODIUM AND IRIDIUM SILICIDES: Ce(Rh,Ir)Si_2, Ce(Rh,Ir)$_2Si_2$, Ce_2(Rh,Ir)$_3Si_5$ AND Ce(Rh,Ir)Si_3

			Lattice parameter (Å)			Average distance (Å)			
Silicide	Structure type	Space group	*a*	*b*	*c*	Ce–*M*	Ce–Si	Ce-valence	Ref.
$CeRhSi_2$	$CeNiSi_2$	*Cmcm*	4.2661(6)	16.758(2)	4.1708(6)	3.235(3)	3.204(3)	IV	[a]
$CeIrSi_2$	$CeNiSi_2$	*Cmcm*	4.2580(7)	16.754(2)	4.1917(7)	3.239(5)	3.206(5)	IV	[a]
$CeRh_2Si_2$	$ThCr_2Si_2$	*I4/mmm*	4.087	4.087	10.17	3.262	3.157	3^+	(*9*)
$CeIr_2Si_2$ (LT)	$ThCr_2Si_2$	*I4/mmm*	4.086(5)	4.086(5)	10.16(1)	3.260	3.156	IV	(*5*)
(HT)	$CaBe_2Ge_2$	*P4/nmm*	4.147(5)	4.147(5)	9.88(1)	3.205	3.185	IV	(*5*)
$Ce_2Rh_3Si_5$	$U_2Co_3Si_5$	*Ibam*	9.874	11.83	5.822	3.245	3.154	IV	(*10*)
$Ce_2Ir_3Si_5$	$U_2Co_3Si_5$	*Ibam*	9.953	11.81	5.804	3.249	3.159	IV	(*10*)
$CeRhSi_3$	$BaNiSn_3$	*I4mm*	4.204	4.204	9.74	3.335	3.177	3^+	(*11*)
$CeIrSi_3$	$BaNiSn_3$	*I4mm*	4.238	4.238	9.784	3.360	3.198	3^+	(*11*)

Note. (The estimated standard deviations are given in parentheses.)
[a] This work.

24.4(3)%; Si: 50.2(3)%) are in agreement with the ideal composition Ce$M$$Si_2$.

The X-ray powder patterns of $CeRhSi_2$ and $CeIrSi_2$ silicides can be indexed with the orthorhombic $CeNiSi_2$-type structure (*3*). Their unit cell parameters are listed in Table I.

The projection of the Ce$M$$Si_2$ structure onto the (0yz) plane is given in Fig. 1. It can be described as a stacking of two different prisms: (i) a trigonal prism [Ce_6] formed by six cerium atoms surrounding a Si(1) atom as, i.e., in binary $CeSi_2$ (*4*); (ii) a distorted antiprism [Ce_4Si_4] surrounding the transition metal Rh or Ir, similar to that found in the high temperature form of $CeIr_2Si_2$ crystallizing in the $CaBe_2Ge_2$-type structure (Fig. 1b) or in the compounds Ce$M$$Si_3$ (M = Rh or Ir) which are isostructural to $BaNiSn_3$ (*5*, *6*). Note also that the crystal structure of the ternary silicides CeM_2Si_2, $Ce_2M_3Si_5$, and Ce$M$$Si_3$ exhibit similar coordination polyhedra for Rh or Ir or Si atoms.

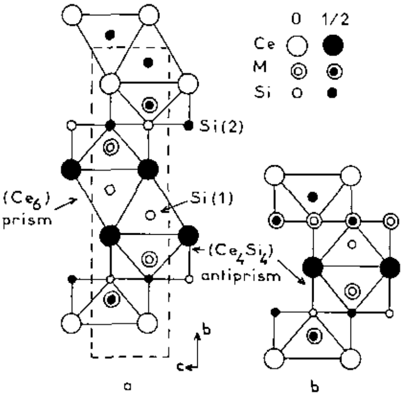

FIG. 1. Crystal structures of Ce$M$$Si_2$ (M = Rh or Ir) (a) and $CeIr_2Si_2$ ($CaBe_2Ge_2$-type) (b) ternary silicides.

The magnetic susceptibility of $CeRhSi_2$ tends to saturate below 70 K whereas that of $CeIrSi_2$ exhibits a broad maximum centered around 110–130 K (Figs. 2 and 3). Such a behavior is commonly observed in intermediate valence systems (*7*). For these two silicides, the sharp increase of the magnetic susceptibility χ_m at low temperatures is attributed to small amounts of stable Ce^{3+} ions stabilized on or near grain boundaries or other lattice defects or to trace of some magnetic impurities. The observed thermal dependence of χ_m can be discussed in terms of a characteristic temperature T_K related to Kondo-type fluctuations (*7*). In this scheme, T_K is defined, below the broad maximum, as

$$T_K = C/2\chi_m(0),$$

where C is the Curie constant for Ce^{3+} ions

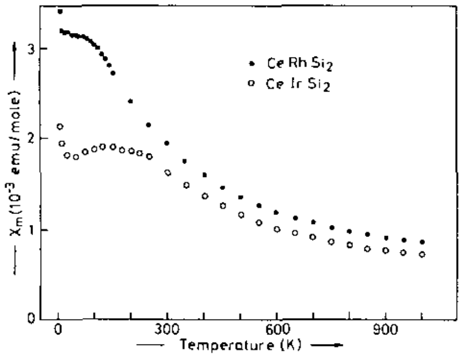

FIG. 2. Temperature dependence of the magnetic susceptibility for $CeMSi_2$ with M = Rh or Ir.

(C = 0.807 emu K/mole) and $\chi_m(0)$ is the magnetic susceptibility at $T = 0$ K. $\chi_m(0)$ is obtained by fitting of χ_m at low temperatures according to (Fig. 3)

$$\chi_m = \chi_m(0) + nC/T,$$

where n is the proportion of stable Ce^{3+} moments composing the trace of magnetic impurities. The values of n, $\chi_m(0)$, and T_K are listed in Table II. We note that T_K ($CeIrSi_2$) > T_K ($CeRhSi_2$) showing that the mixing between $4f$(Ce) and conduction band states is more pronounced in $CeIrSi_2$ than in $CeRhSi_2$. This fact is certainly due to a broadening of the conduction band induced by a better overlapping of the d-orbitals when the rhodium $4d$-metal is replaced by the iridium $5d$-metal.

Above the broad maximum, the spin fluctuation temperature T_K^* is defined as the temperature such that (7):

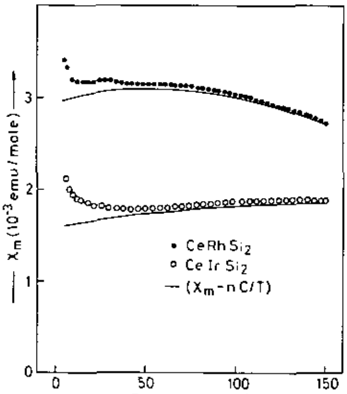

FIG. 3. Measured and corrected ($\chi_m - nC/T$) magnetic susceptibility versus temperature for $CeMSi_2$ with M = Rh or Ir.

$$T_K^* \chi_m(T_K^*) = C/2.$$

For these two ternary silicides, the T_K^* values are given in Table II. Let us note that the T_K and T_K^* values are in agreement. Moreover the corrected magnetic susceptibility (χ_m-nC/T), shown in Fig. 3 goes through a maximum near 62(5) K and 110–130 K respectively for $CeRhSi_2$ and $CeIrSi_2$. These temperatures are consistent with the model offered by Lawrence *et al.* which forecasts that the thermal dependence of the susceptibility exhibits a maximum above $T = T_K/2$ (7). We also note that the spin fluctuation temperature of $CeIrSi_2$ is intermediate between that observed for the two crystallographic forms of the intermediate valent cerium silicide $CeIr_2Si_2$ (Table II) (5, 8).

TABLE II

SPIN FLUCTUATION TEMPERATURES T_K AND T_K^* AND AVERAGE DISTANCE Ce–(Rh,Ir) FOR THE CERIUM SILICIDES $Ce(Rh,Ir)Si_2$ AND $CeIr_2Si_2$

Silicide	n (10^{-2}Ce atom/mole)	$\chi_m(0)$ (10^{-3} emu/mole)	$T(\chi_{max})$ (K)	T_K (K)	T_K^* (K)	(Ce–M) distance (Å)
$CeRhSi_2$	0.31	3.02	62(5)	134(5)	143(5)	3.235(3)
$CeIrSi_2$	0.37	1.62	110–130	249(8)	225(8)	3.239(5)
$CeIr_2Si_2$(HT)	0.5	1.3	–	311(8)	>280	3.205(6)
$CeIr_2Si_2$(LT)	0.95	1.92	120(10)	209(7)	180(7)	3.260(6)

For $CeRhSi_2$, the electrical resistivity remains practically constant between 270 K and 150 K then decreases with decreasing temperature (Fig. 4). On the other hand, the resistivity of $CeIrSi_2$ decreases in the temperature range considered but shows a curvature at higher temperatures ($T > 140$ K). This behavior is characteristic for an intermediate valent compound having a high spin fluctuation temperature such as $CeIr_2Si_2$ (HT) (*5*).

The valence state of cerium in the ternary silicides $Ce_xM_ySi_z$ (M = Rh or Ir) depends on the average distance Ce–M which determines the strength of the $4f$(Ce)–$4d$ or –5d(M) hybridization (Fig. 5 and Tables I and II). An increase of the Ce–M distance induces a transition for the Ce-atom from an intermediate valence state to a trivalent state. For instance with M = Rh and increasing distance, the Ce-atom has an intermediate valence state in $CeRhSi_2$ [112] and $Ce_2Rh_3Si_5$ [235], whereas it is purely trivalent in $CeRh_2Si_2$ [122] and $CeRhSi_3$ [113] (Fig. 5). Recently we have shown that the Ce-atom has an intermediate valence state in the $Ce(Rh_{1-x}Co_x)_2Si_2$ solid solution for $x \geq 0.135$, that is to say for a (Ce–Rh) distance $\leq 3.254(4)$ Å (*9*). This distance could be a critical distance determining the valence state of Ce-atoms in the ternary silicides $Ce_xRh_ySi_z$. It is interesting to note that the spin fluctuation temperature T_K increases when the Ce–Rh distance d decreases: $Ce(Rh_{0.865}Co_{0.135})_2Si_2$ [T_K = 90 K and d = 3.254(4) Å] and $CeRhSi_2$ [T_K = 134 K and d = 3.235(3) Å].

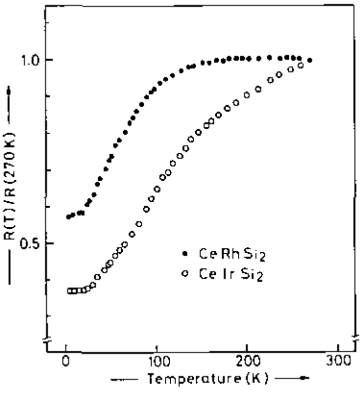

FIG. 4. Temperature dependence of the reduced electrical resistivity for $CeMSi_2$ with M = Rh or Ir.

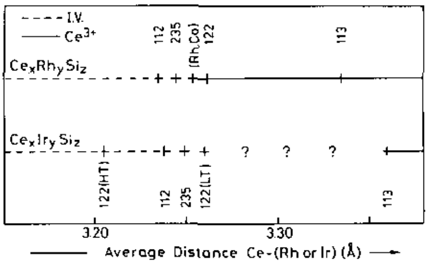

FIG. 5. Cerium valence versus average distance Ce–M in the ternary silicides CeM_2Si_2 [122], $CeMSi_2$ [112], $Ce_2M_3Si_5$ [235], and $CeMSi_3$ [113] with M = Rh or Ir.

For M = Ir, the Ce-atom has an intermediate valence state in the ternary silicides for Ce–Ir distances at least lower than 3.260 Å (for instance in $CeIr_2Si_2$ (HT), $Ce_2Ir_3Si_5$, and $CeIr_2Si_2$ (LT)) (Fig. 5). In the absence of sufficient crystallographic data concerning these compounds no critical distance can be determined. Let us also note that the T_K temperature increases with decreasing Ce–Ir distances. $CeIrSi_2$ exhibits both T_K and Ce–Ir distance values intermediate between that observed for the two crystallographic forms (LT) and (HT) of $CeIr_2Si_2$ (Table II).

Acknowledgments

The authors (B.C. and P.R.) are both grateful to the CNRS and the Austrian Academy of Sciences for research stipends at the Universities in Bordeaux and Vienna. Part of this research has been supported by the Austrian FFWF (Project 8218) which is gratefully acknowledged.

References

1. B. CHEVALIER, P. LEJAY, J. ETOURNEAU, AND P. HAGENMULLER, *Mater. Res. Bull.* **18,** 315 (1983).

2. H. F. BRAUN, *J. Less-Common Met.* **100,** 105 (1984).

3. O. P. BODAK AND E. I. GLADYSHEVSKII, *Sov. Phys. Crystallogr.* **14,** 859 (1970).

4. P. VILLARS AND L. D. CALVERT, "Pearson's

Handbook of Crystallographic Data," 2nd ed., and "Atlas of Crystal Structure Types," ASM, Materials Park, OH (1991).

5. B. BUFFAT, B. CHEVALIER, M. H. TUILIER, B. LLORET, AND J. ETOURNEAU, *Solid State Commun.* **59,** 17 (1986).
6. B. CHEVALIER, P. LEJAY, B. LLORET, WANG-XIAN-ZHONG, J. ETOURNEAU, AND P. HAGENMULLER, *Ann. Chim. Fr.* **9,** 987 (1984).
7. J. M. LAWRENCE, P. S. RISEBOROUGH, AND R. D. PARKS, *Rep. Prog. Phys.* **44,** 1 (1981).
8. B. LLORET, Thesis, Université de Bordeaux I, (1988).
9. B. CHEVALIER, J. ETOURNEAU, J. ROSSAT-MIGNOD, R. CALEMECZUK, AND E. BONJOUR, *J. Phys. Condens. Matter* **3,** 1847 (1991).
10. C. GODART, C. V. TOMY, L. C. GUPTA, AND R. VIJAYARAGHAVAN, *Solid State Commun.* **67,** 677 (1988).
11. P. HAEN, P. LEJAY, B. CHEVALIER, B. LLORET, J. ETOURNEAU, AND M. SERA, *J. Less-Common. Met.* **110,** 321 (1985).